



**HAL**  
open science

## TDMQ20, a Specific Copper Chelator, Reduces Memory Impairments in Alzheimer's Disease Mouse Models

Jie Zhao, Qihui Shi, Hongda Tian, Youzhi Li, Yan Liu, Zhen Xu, Anne Robert, Qiong Liu, B. Meunier

### ► To cite this version:

Jie Zhao, Qihui Shi, Hongda Tian, Youzhi Li, Yan Liu, et al.. TDMQ20, a Specific Copper Chelator, Reduces Memory Impairments in Alzheimer's Disease Mouse Models. ACS Chemical Neuroscience, 2021, 12 (1), pp.140-149. 10.1021/acchemneuro.0c00621 . hal-03079460

**HAL Id: hal-03079460**

**<https://hal.science/hal-03079460>**

Submitted on 17 Dec 2020

**HAL** is a multi-disciplinary open access archive for the deposit and dissemination of scientific research documents, whether they are published or not. The documents may come from teaching and research institutions in France or abroad, or from public or private research centers.

L'archive ouverte pluridisciplinaire **HAL**, est destinée au dépôt et à la diffusion de documents scientifiques de niveau recherche, publiés ou non, émanant des établissements d'enseignement et de recherche français ou étrangers, des laboratoires publics ou privés.

1  
2 **TDMQ20, a specific copper chelator, reduces memory impairments in AD-**  
3 **mouse models**

4  
5 Jie Zhao, Qihui Shi, Hongda Tian, Youzhi Li, Yan Liu, Zhen Xu, Anne Robert,\* Qiong Liu,\*  
6 Bernard Meunier\*

7  
8 ABSTRACT

9  
10 Beside targeting amyloid or tau metabolisms, regulation of redox metal ions is a recognized  
11 therapeutic target for Alzheimer's disease (AD). Based on the bioinorganic chemistry of copper,  
12 we designed specific chelators of copper(II) (TDMQs) in sight to regulate copper homeostasis in  
13 the brain, and to inhibit the deleterious oxidative stress catalyzed by copper-amyloid complexes.  
14 An oral treatment by TDMQ20 was able to fully reverse the cognitive and behavioral impairment  
15 in three different murine models, two non-transgenic models mimicking the early stage of AD,  
16 and a transgenic representing a more advanced stage of AD. To our knowledge, such comparative  
17 study using the same molecule has never been performed.

18 Regular C57 BL/6J mice received a single injection of human Cu-A $\beta$ <sub>1-42</sub> in the lateral ventricles  
19 (icv-CuA $\beta$ ) or in the hippocampus (hippo-CuA $\beta$ ). In both cases, mice developed a cognitive  
20 impairment similar to that of transgenic 5XFAD mice. Oral administration of TDMQ20 to icv-  
21 CuA $\beta$  or hippo-CuA $\beta$  mice within a 16-days period resulted in a significant improvement of the  
22 cognitive status. The 3-months treatment of transgenic 5XFAD mice with TDMQ20 also resulted  
23 in behavioral improvements. The consistent positive pharmacological results obtained using these  
24 different AD models correlate well with previously obtained physico-chemical data of TDMQ20.  
25 The short-term novel object recognition (NOR) test was found particularly relevant to evaluate  
26 the rescue of declarative memory impairment. TDMQ20 was also able to reduce the oxidative  
27 stress in the mouse cortex. Due to its reliability and facile use, the hippo-CuA $\beta$  model can be  
28 considered as a robust non-transgenic model to evaluate the activity of potential drugs on the early  
29 stages of memory deficits.

30  
31 KEYWORDS

32 Alzheimer's disease / copper / chelator / memory / mouse models / hippocampus

33

## 34 1. INTRODUCTION

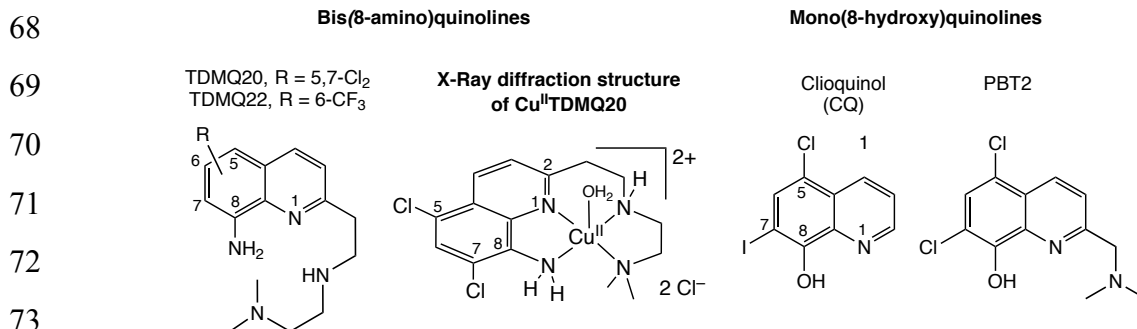
35

36 Alzheimer's disease (AD) affects millions of people worldwide, and the incidence of this age-  
37 related disease is increasing due to the increase of life expectancy in many countries.<sup>1,2</sup> AD being  
38 mainly characterized by the formation of senile plaques of  $\beta$ -amyloid peptides and by  
39 neurofibrillary tangles due to the hyperphosphorylation of the tau protein, these phenomena have  
40 been considered as targets for the design of therapeutic agents.

41 Since memantine in 2003, no new drug has been approved, except sodium oligomannate (GV-  
42 971), recently approved by the National Medical Products Administration of China.<sup>3</sup> Between  
43 2003 and 2019, 100 % of drug-candidates failed in clinical trials.<sup>4</sup> The quasi-exclusive use of  
44 transgenic mice to select drug-candidates for a disease which has no genetic origin for sporadic  
45 cases, might be questioned. Predictive and easy to handle mouse AD models are needed. In an  
46 attempt of diversification, we developed a non-transgenic mice model for the evaluation of the  
47 chelator PA1637.<sup>5</sup> In this model, an episodic memory deficit was generated by a single  
48 intracerebroventricular (icv) injection in the brain of normal mice, of low molecular weight  $A\beta_{1-42}$   
49 oligomers without copper. Despite controversies on the role of soluble amyloids,<sup>6</sup> they are still  
50 considered as toxic agents contributing to synaptic alteration, abnormal tau phosphorylation, glial  
51 activation and neuronal loss *in vivo*.<sup>7</sup> More recently, the key role of  $A\beta$  oligomers to trigger  
52 activation of the glycogen synthase kinase 3 $\beta$  (GSK3 $\beta$ ), responsible for tau hyperphosphorylation,  
53 has been demonstrated.<sup>8</sup>

54 Despite the capacity of PA1637 to extract copper from copper-amyloid *in vitro*, and to inhibit  
55 the catalytic production of  $H_2O_2$  by Cu(II)-amyloid<sup>9,10</sup> its development has been stopped due to  
56 its rather low bioavailability. Consequently, we designed a new series of specific chelators of  
57 Cu(II) named TDMQ, based on a 8-aminoquinoline skeleton with a chelating side-chain at C2  
58 (Figure 1). Such tetradentate ligands have the required structure to discriminate between copper  
59 and zinc.<sup>11-15</sup> Two 8-hydroxyquinolines, clioquinol (CQ) and PBT2, failed in clinical trials to  
60 improve cognition and reduce amyloid plaques.<sup>16,17</sup> This failure might be explained by their lack  
61 of specificity for copper chelation,<sup>18,19</sup> and their inability to inhibit the production of reactive  
62 oxygen species (ROS) generated by the Cu-amyloids.<sup>15,20</sup> TDMQ ligands are able to extract  
63 copper(II) from Cu-amyloids, without disturbing the activities of Cu,Zn-SOD, tyrosinase or  
64 vitamin B<sub>12</sub>.<sup>14</sup> TDMQ20 has been selected as lead molecule for evaluation as anti-AD drug-  
65 candidate on three different mouse models, two non-transgenic- and a transgenic one. TDMQ22,

66 a second chelator, differs from TDMQ20 by having a  $\text{CF}_3$  substituent at position 6 instead of Cl  
 67 at C5 and C7.<sup>13</sup>



75 **Figure 1.** Structure of the chelators TDMQ20, TDMQ22, clioquinol (CQ) and PBT2, and structure of the copper(II)  
 76 complex of TDMQ20, for its X-ray structure data, see Reference 11.

77

78 The deregulation of copper in AD brain and the associated memory deficits have been created  
 79 by injection of the copper complex of amyloid  $\text{A}\beta_{1-42}$  in the lateral ventricles (icv-Cu $\text{A}\beta$  model)  
 80 or hippocampus (hippo-Cu $\text{A}\beta$  model) of regular mice. The third model was the transgenic mouse  
 81 5XFAD model. Data obtained with these three murine models indicated that the oral  
 82 administration of TDMQ20 was able to inhibit memory deficits.

## 84 2. RESULTS AND DISCUSSION

### 86 2.1. Mouse AD models, and drug treatment.

87 In two non-transgenic mouse models, the cognitive deficit was created by injection of human Cu<sup>II</sup>-  
 88  $\text{A}\beta_{1-42}$  complex either in the lateral ventricles (icv-Cu $\text{A}\beta$  model) or in the hippocampus (hippo-  
 89 Cu $\text{A}\beta$  model) of regular young C57BL/6J mice (two months of age), at D0. The icv-Cu $\text{A}\beta$  model  
 90 of AD is similar to the icv injection of  $\text{A}\beta_{1-42}$  oligomers used to evaluate the tetradentate PA1637  
 91 chelator.<sup>5</sup> In the second non-transgenic model, hippo-Cu $\text{A}\beta$ , the Cu- $\text{A}\beta_{1-42}$  solution was injected  
 92 in the hippocampus. This region of the brain is involved in declarative memory and learning as  
 93 well as in spatial memory, and is particularly vulnerable in the early stages of AD.<sup>21,22</sup> Atrophy  
 94 of hippocampus is strongly correlated with cognitive decline.<sup>23</sup> This non-transgenic hippo-Cu $\text{A}\beta$   
 95 model can therefore contribute to mimic the early stages of AD.

96 In these non-transgenic AD mice, the drug treatment consisted of oral gavage with TDMQ20,  
 97 TDMQ22 or CQ used as comparator, 8 times between D4 and D20 (each dose was 10 mg kg<sup>-1</sup>).

98 We also evaluated TDMQ20 on the transgenic 5XFAD transgenic mouse model (C57BL6  
 99 genetic background), that expressed human APP and PSEN1 transgenes with a total of five AD-

100 linked mutations: the Swedish (K670N/M671L), Florida (I716V) and London (V717I) mutations  
101 in APP (the precursor of amyloids) and the two mutations in PSEN1 (M146L and L286V) (PSEN1  
102 is the gene coding for presenilin-1, a constituent of  $\gamma$ -secretase). This model recapitulates several  
103 AD-related aspects of the disease,<sup>24,25</sup> with early formation of amyloid plaques and gliosis at two  
104 months. Cognitive and motor deficits start at about 6 months, and develop with age in parallel  
105 with neuron degeneration in multiple brain regions.<sup>26,27</sup>

106 For 5XFAD mice, the drug treatment was carried out once every two days, from 2 to 5 months  
107 of age, and consisted of oral gavage with TDMQ20, or CQ used as comparator, (45 times, each  
108 drug dose: 10 mg kg<sup>-1</sup>). The mouse cognitive status was evaluated using the standardized  
109 behavioral tests: novel object recognition (NOR), elevated plus maze test (EPM), open field test  
110 (OFT), and Y-maze test (YMT), at the end of the treatment (between D22 and D26 for the icv-  
111 CuA $\beta$  model and the hippo-CuA $\beta$  model), and between 5.2 and 5.6 months of age for the 5XFAD  
112 mice.

113

## 114 **2.2. TDMQ20 inhibits of the cognitive impairment of AD mice.**

### 115 **2.2.1. Novel object recognition (NOR)**

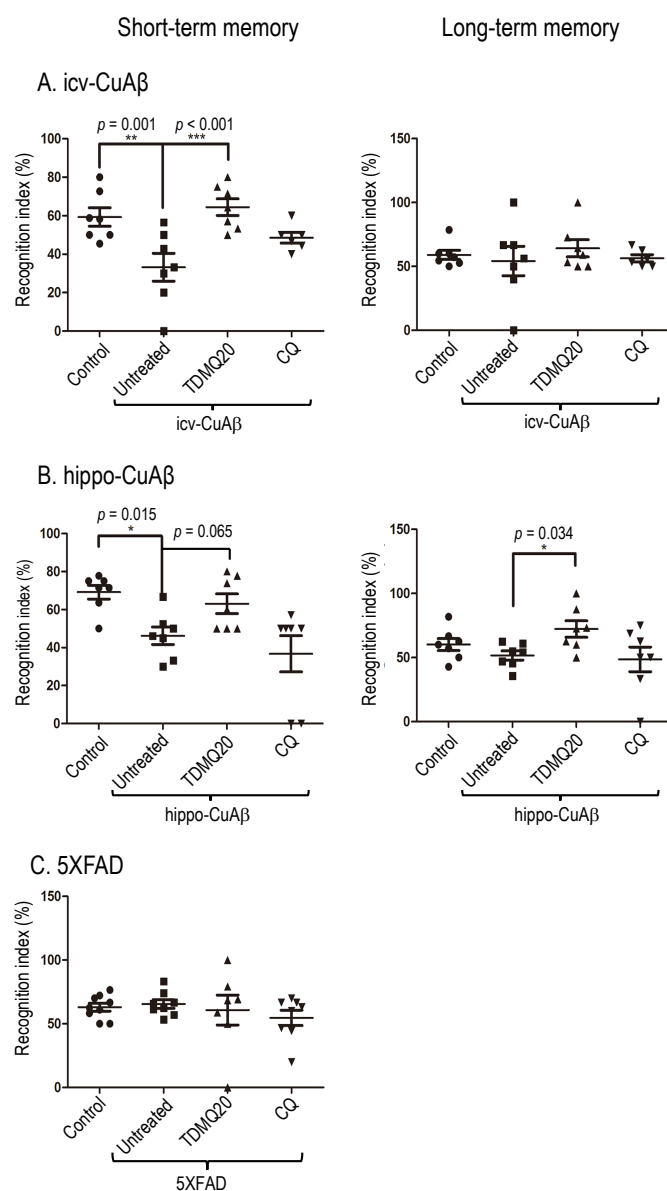
116 The NOR test, based on the spontaneous propensity of rodents to explore new objects, allows the  
117 evaluation of short-term- or long-term memory,<sup>28</sup> assessing cognitive deficits in a wide range of  
118 pathological conditions, in transgenic and non-transgenic murine models of AD.<sup>29</sup> This assay is  
119 particularly relevant to AD, and consequently for the evaluation of the efficacy of potential drugs  
120 since it is dependent on the integrity of the temporal regions affected in the early stages of AD.

121 The recognition index is calculated as the percentage of explorations of a novel object with  
122 respect to the total number of explorations for short-term memory or long-term memory  
123  $\{[(n_Y/n_{X+Y}) \times 100]$  or  $[(n_Z/n_{X+Z}) \times 100]$ , respectively, where  $n_X$ ,  $n_Y$ ,  $n_Z$  stand for the number of  
124 explorations of familiar object X, novel object Y in short-term memory evaluation, or novel object  
125 Z in long-term memory evaluation, respectively}. The recognition index is reported in Figure 2  
126 for the icv-CuA $\beta$  (panel A), the hippo-CuA $\beta$  (panel B), and the 5XFAD (panel C) mouse models.

127 First of all, for short-term memory evaluation, the recognition index was significantly lower  
128 for the icv-CuA $\beta$  mice or hippo-CuA $\beta$  mice compared to the healthy controls (Figure 2, panel A  
129 or B, respectively), indicating that this test was relevant to discriminate between healthy and non-  
130 transgenic AD mice, a necessary condition to evaluate the activity of potential drugs on these  
131 models. Contrary, the difference of the recognition index was not statistically significant between

132 5XFAD mice and their wild type littermates (panel C), consistent with bibliographic data  
 133 indicating that, in transgenic models of AD, the performance of mice in the NOR is age-dependent  
 134 and deficits appear only after 6 months of age,<sup>29</sup> or even later.<sup>30</sup>

135 This result suggests that icv-CuA $\beta$ - and hippo-CuA $\beta$  mice are mimicking early cognitive  
 136 impairment of AD, whereas such damages are probably undetectable in young 5XFAD mice.



157  
 158  
 159 **Figure 2.** Declarative memory evaluated by the recognition index  $[(n_Y/n_{X+Y}) \times 100]$  for short term memory or  
 160  $[(n_Z/n_{X+Z}) \times 100]$  for long-term memory in the NOR task in the icv-CuA $\beta$  (panel A) and the hippo-CuA $\beta$  (panel B)  
 161 non-transgenic mouse models, and in the transgenic 5XFAD (panel C) model.  $n_X$ ,  $n_Y$ ,  $n_Z$  stand for the number of  
 162 explorations of familiar object X, novel object Y in short-term memory evaluation, or novel object Z in long-term  
 163 memory evaluation, respectively. In each case, the recognition index of AD mice which received no drug-treatment  
 164 (untreated group) was compared to that of healthy mice (control group), and to the recognition index of AD mice  
 165 treated with TDMQ20 or clioquinol [ $8 \times 10 \text{ mg kg}^{-1}$  in 16 days (panels A and B), or  $10 \text{ mg kg}^{-1}$ , one every two days  
 166 during 3 months (panel C)]. In panels A or B, the control/untreated groups were brain-injected with CuA $\beta$ /PBS. In  
 167 panel C, the untreated and control groups were the transgenic 5XFAD mice and their non-transgenic littermates  
 168 (C57BL6), respectively. All control and untreated mice received oral gavage with aqueous NaCl 0.9 w/v instead of  
 169 drug. For details, see SI. Each mark represents the result obtained with a single mouse; horizontal lines represent

170 mean values  $\pm$  SEM [panels A and B: n = 7 (controls) or 6-7 (untreated- or treated AD mice); panel C: n = 9 (controls)  
171 or 7-8 (untreated- or treated 5XFAD mice)].  $^{***}p < 0.01$ ,  $^{*}p < 0.05$  vs. the untreated AD group (ANOVA).

172 After a short oral treatment by TDMQ20 icv-CuA $\beta$  mice spent significantly more time  
173 exploring the novel object in the short-term memory test, compared to untreated AD mice. A  
174 similar trend was evidenced for hippo-CuA $\beta$  mice. In fact, the recognition index of treated mice  
175 was similar to the score of control mice. Then, TMDQ20 significantly reduced the cognitive  
176 injuries created by the intracerebral injection of the Cu-A $\beta_{1-42}$  complex. By comparison, CQ did  
177 not significantly improved the short-term memory of icv-CuA $\beta$  mice and hippo-CuA $\beta$  mice.  
178 Duplication of these experiments using icv-CuA $\beta$ - and hippo-CuA $\beta$  mice provided fully  
179 consistent results provided as Supporting Information (Figure S1). The ability of TDMQ22 to  
180 restore the short-term memory of icv-CuA $\beta$  mice was close to that of TDMQ20 (SI, Figure S1,  
181 panel A).

182 Contrary to the short-term memory, the long-term recognition index was not significantly  
183 impaired in icv-CuA $\beta$ - and hippo-CuA $\beta$  mice (panels A and B, right). This result suggests that  
184 these models efficiently mimic the early stage of AD, in which the short-term memory is the first  
185 to be impaired, while the long-term memory, including semantic and procedural memories are not  
186 yet significantly impacted. We should note that the development of efficient drugs requires the  
187 use of mouse models of the early stages of the disease, and not a model for the late stages, where  
188 cognitive and anatomic damages are irreversible.

### 189 **2.2.2. Y-maze test**

190 The Y-maze test is a measure of spatial working memory driven by the innate curiosity of rodents  
191 to explore previously unvisited areas.<sup>31</sup> The spontaneous alternation of mice in the Y-maze has  
192 been validated as a hippocampal relevant spatial task.<sup>32,33</sup> The spontaneous alternation ratios of  
193 hippo-CuA $\beta$ - and 5XFAD mice in the Y-maze are reported in Figure 3, panels A and B,  
194 respectively. The 5XFAD mice exhibit a tendency to reduced spontaneous alternation ratio  
195 compared with wild-type mice (Figure 3), consistent with previous reports indicating that  
196 alternation ratio was impaired after the age of 6 months.<sup>24,25</sup> The oral treatment by TDMQ20  
197 restored the alternation ratio of 5XFAD mice (panel B) up to the level of control mice, with nearly  
198 the same efficacy than CQ. A similar trend was obtained with hippo-CuA $\beta$  mice. Due to the result  
199 lack of statistical significance, we suggest that the spatial memory impairment is not yet  
200 established in these non-transgenic early AD mice. Therefore this test is poorly suitable to  
201 evaluate the cognitive impairment and the efficacy of drugs in 2-3 month old hippo-CuA $\beta$  mice.

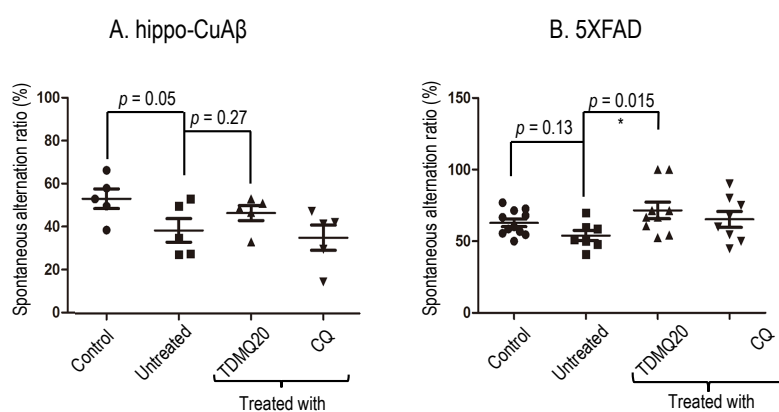


**Figure 3.** Spatial memory evaluated by the spontaneous alternation ratio in the in the Y-maze task for the hippo-CuA $\beta$  (panel A) non-transgenic mouse model, and the transgenic 5XFAD (panel B) model. In each case, the spontaneous alternation rate of AD mice which received no drug-treatment (untreated group) was compared to that of healthy mice (control group), and to the alternation ratio of AD mice which received TDMQ20 or cloioquinol ( $8 \times 10 \text{ mg kg}^{-1}$  in 16 days, panel A, or  $10 \text{ mg kg}^{-1}$ , one every two days during 3 months, panel B). In panel A, the control/untreated groups were brain-injected with CuA $\beta$  in PBS. In panel B, the untreated and control groups were the transgenic 5XFAD mice and their non-transgenic littermates, respectively. All control and untreated mice received oral gavage with aqueous NaCl 0.9 w/v instead of drug. For details, see SI. Each mark represents the result obtained with a single mouse; horizontal lines represent mean values  $\pm$  SEM [(A):  $n = 5$ ; (B):  $n = 9$  (controls) or 7-8 (untreated- or treated 5XFAD mice)].  $p$  values in the ANOVA are indicated.

### 2.2.3. Open field test

In the open-field assay, the unsupported rearings and travel distances of the hippo-CuA $\beta$  mice in the open-field were found significantly lower than that of age-matched controls, indicating that the locomotor deficit of hippo-CuA $\beta$  mice was well established (Figure 4A). Here also, the treatment by TDMQ20 for a short period of 16 days resulted in full rescue of the mouse abilities, with both rearings and travel distances similar to that of controls.

Conversely, the locomotor activity of 5XFAD mice was found rather close to that of the corresponding healthy mice, with no significant difference in the rearings between WT and 5XFAD mice (Figure 4B). This is consistent with the fact that the exploratory behavior and locomotor activity of 5XFAD mice were reported as being normal at least until 6 months,<sup>26,27</sup> or 9-12 months old.<sup>25,30</sup> However, in our hands, the grid crossings by 5XFAD animals was significantly higher than that of their WT littermates (Figure 4B), suggesting that, at 5.4 months, brain damage were already installed. In these conditions, the treatment by TDMQ20 significantly normalized the grid crossing by transgenic AD mice.



241  
242  
243  
244  
245  
246  
247  
248  
249  
250  
251  
252  
253  
254  
255  
256  
257  
258  
259  
260  
261  
262  
263  
264  
265  
266  
267  
268  
269  
270  
271  
272  
273  
274  
275  
276

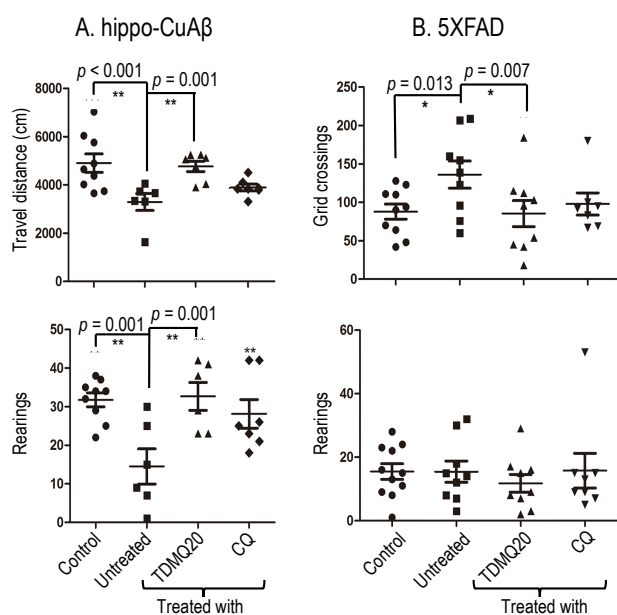


**Figure 4.** Locomotion ability evaluated by the crossings, travel distances, and rearings, in the open field test for the hippo-CuA $\beta$  (panel A) non-transgenic mouse model, and the transgenic 5XFAD (panel B) model. In each case, the scores of AD mice which received no drug-treatment (untreated group) was compared to that of healthy mice (control group), and to the scores of AD mice which received TDMQ20 or clioquinol ( $8 \times 10 \text{ mg kg}^{-1}$  in 16 days, panel A, or  $10 \text{ mg kg}^{-1}$ , one every two days during 3 months, panel B). In panel A, the control/untreated groups were brain-injected with CuA $\beta$  in PBS. In panel B, the untreated and control groups were the transgenic 5XFAD mice and their non-transgenic littermates, respectively. All control and untreated mice received oral gavage with aqueous NaCl 0.9 w/v instead of drug. For details, see SI. Each mark represents the result obtained with a single mouse; horizontal lines represent mean values  $\pm$  SEM. [(A):  $n = 9$  (control), or 6-7 (untreated or treated hippo-CuA $\beta$  mice; (B):  $n = 10$  (control), or 7-9 (untreated or treated 5XFAD mice)]. \*\*\* $p < 0.001$ , \*\* $p < 0.01$ , \* $p < 0.05$  vs. untreated AD mice (ANOVA).

#### 2.2.4. Elevated plus maze

The elevated plus maze assay has been described for assessing anxiety response of rodents, and screening of drugs for treatment of anxiety-related disorders.<sup>34,35</sup> The score of 5XFAD mice in the elevated plus maze is reported in Figure 5. 5XFAD mice exhibited an increased number of closed arm entries, and a decreased proportion of time spent in closed arms, compared to their WT littermates. Normally, mice tend to avoid the open arms, seeking protection in the closed arms. A decreased proportion of time spent in closed arms indicate a decreased anxiety of 5XFAD mice (Figure 5), that may correspond to dis-inhibitory tendencies seen in AD patients.<sup>25,26</sup> Oral treatment of these mice with TDMQ20 fully reversed their behavior to to the score of WT, more efficiently than the CQ treatment did.

277  
 278  
 279  
 280  
 281  
 282  
 283  
 284  
 285  
 286  
 287  
 288  
 289  
 290  
 291  
 292  
 293  
 294  
 295  
 296  
 297  
 298  
 299  
 300  
 301  
 302  
 303  
 304  
 305  
 306  
 307  
 308  
 309  
 310  
 311  
 312  
 313

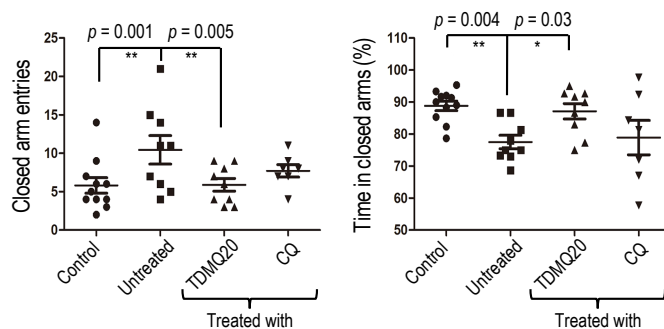


**Figure 5.** Anxiety evaluated by the closed arm entries and time spent in closed arms, in the elevated plus maze test for the transgenic 5XFAD model. The scores of AD mice which received no drug-treatment (untreated group) was compared to that of wild-type mice (control group), and to that of AD mice which received TDMQ20 or clioquinol ( $10 \text{ mg kg}^{-1}$ , one dose every two days during 3 months). The untreated and control groups were the transgenic 5XFAD mice and their non-transgenic littermates, respectively. All control and untreated mice received oral gavage with aqueous NaCl 0.9 w/v instead of drug. For details, see SI. Each mark represents the result obtained with a single mouse; horizontal lines represent mean values  $\pm$  SEM. (controls:  $n = 9$ ; untreated- or treated 5XFAD mice:  $n = 7-8$ ). \*\*\* $p < 0.001$ , \*\* $p < 0.01$ , \* $p < 0.05$  vs. the untreated 5XFAD mice (ANOVA).

As a summary of behavioral tests (Table 1), both 2.5-2.7 month hippo-CuA $\beta$  or icv-CuA $\beta$  mice exhibited significant deficits of short-term memory in the NOR assay. The score of the hippo-CuA $\beta$  mice was also impaired in the open-field assay, validating these non-transgenic models to evaluate the activity of potential drugs on the early stages of the memory deficits. The short oral treatment with TDMQ20 was efficient to fully restore the abilities of mice in these reference tests. The score of hippo-CuA $\beta$  mice in the Y-maze was less impaired than in transgenic 5XFAD mice, but nevertheless confirmed that TDMQ20 was able to reverse the ongoing impairment of the spatial memory on young mice affected by intracerebral injection of copper-amyloids.

Conversely, the deficits of 5XFAD mice observed in the open field, Y-maze or elevated plus maze assays, are rather weak below 6 months of age. Cognitive deficits of these transgenic mice are reported to correlate well with an increasing burden of amyloid plaques in the cortex and hippocampus, axonal degeneration, spinal cord pathology and neuron loss in specific cortical layer, mimicking an advanced AD pathology.<sup>25</sup> Similarly, in APP/PS-1 mouse model, the cognitive deficits in both recognition memory and spatial memory become apparent only at 11-24 months of age, when the disease damages are definitively installed.<sup>36</sup> In these conditions, such transgenic models should be considered more relevant to describe advanced stages of AD, but are probably not really adapted to evaluate drug-candidates that should be efficient on the early stages of the disease.

**Table 1.** Improvement of the scores of AD mice treated by TDMQ20, with respect to untreated AD controls.

		AD mouse model		
		icv-CuA $\beta$	hippo-CuA $\beta$	5XFAD
Behavioral test	NOR (short term)	++ <sup>a</sup>	++	nr <sup>d</sup>
	Y-maze	nd <sup>c</sup>	+ <sup>b</sup>	+ <sup>b</sup>
	Open field	nd	++	+ <sup>b,e</sup>
	Elevated plus maze	nd	nd	++
Cortex oxidative status	MDA level	+ <sup>b</sup>	nd	+ <sup>b</sup>

<sup>a</sup> ++ Means: Statistically significant with  $p$ -value  $\leq 0.05$  (ANOVA); <sup>b</sup> + Means: tendency, but with  $p$ -value  $> 0.05$ ; <sup>c</sup> nd Not determined; <sup>d</sup> Not relevant (no significant difference between WT controls and 5-month old 5XFAD mice); <sup>e</sup> Only for grid crossing.

### 2.3. TDMQ20 inhibits cortex oxidative injuries

The ability of TDMQ20 to rescue cognitive deficits is consistent with the capacity of this copper homeostasis regulator to reduce *in vitro* the formation of ROS.<sup>13,20</sup> In fact, neuro-inflammation is considered a key factor of the loss of neurons and synapses in AD.<sup>30</sup> The molecular origin of brain inflammation might be linked to the oxidative stress initiated by the reductive activation of dioxygen catalyzed by copper-amyloids. It is therefore relevant to evaluate the oxidative status of the mouse brains. For this purpose, the malondialdehyde (MDA) level is significant of the potential occurrence of peroxide induced lipid injuries.<sup>37</sup>

The level of MDA, measured by the thiobarbituric reactive species (TBARS) assay, in the cortex of icv-CuA $\beta$ - and 5XFAD mice is reported in Figure 6A and 6B, respectively.

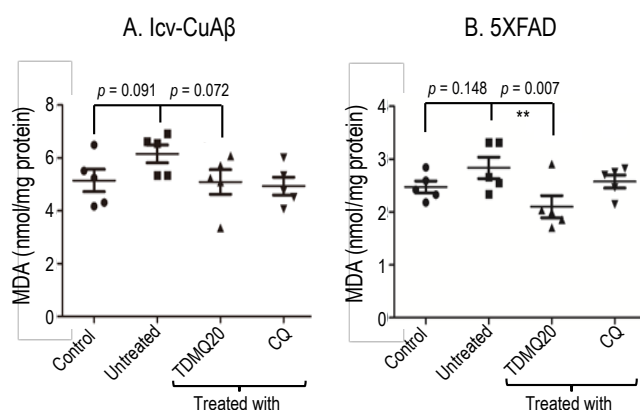


**Figure 6.** Effect of TDMQ20 on the level of malondialdehyde in the cortex of icv-CuA $\beta$  AD mice (A) and 5XFAD mice (B). (A): The control mice were brain-injected with PBS 1X/DMSO, 80/20, v/v; untreated mice were brain injected with CuA $\beta$  in 1X/DMSO, 80/20, v/v. (B): The controls were WT C57BL/6J mice. All control and untreated

353 mice received oral gavage with aqueous NaCl 0.9 w/v instead of drug. Each mark represents the result obtained with  
 354 a single mouse; horizontal lines represent mean values  $\pm$  SEM of  $n = 5$  experiments. Relevant  $p$  values are indicated  
 355 (ANOVA).

356 The concentration of MDA in the cortex of AD mice, transgenic (5XFAD) or not (icv-CuA $\beta$ ),  
 357 was slightly higher than that of the controls (Figure 6), supporting the involvement of an oxidative  
 358 stress in these mice. In both cases, the treatment with TDMQ20 reduced the MDA level in the  
 359 cortex until the level of control mice, indicating a normalization of the oxidative status in the  
 360 cortex. This encouraging data is consistent with the ability of TDMQ20 to inhibit *in vitro* the  
 361 production of ROS induced by Cu-A $\beta$ .<sup>13,15</sup>

362

## 363 2.4. Preliminary safety and druggability studies of TDMQ20

### 364 2.4.1. Single dose

365 In an acute toxicity assay in WT C57BL/6J mice, TDMQ20 was found completely safe after  
 366 administration of an oral dose 150 or 200 mg kg<sup>-1</sup>, corresponding to 15-20 times the dose used to  
 367 treat AD mice, with all mice surviving without any detectable deficit (Table 2). The drug exhibited  
 368 some delayed toxicity by ip route at 150 mg kg<sup>-1</sup>: two mice over 11 died at D3 and D15,  
 369 respectively, indicating an LD<sub>50</sub> value higher than 150 mg kg<sup>-1</sup>. By comparison, clioquinol was  
 370 found significantly more toxic, with LD<sub>50</sub> values close to 200 mg kg<sup>-1</sup> and 150 mg kg<sup>-1</sup>, by oral  
 371 and ip route, respectively (2/5 and 7/11 mice died on the day of drug administration).

372

373 **Table 2.** Preliminary toxicological evaluation of TDMQ20 compared to CQ on C57BL/6J mice, after a single oral or  
 374 intraperitoneal (ip) dose.

375 Survival of mice treated with a single dose of TDMQ20 or CQ

Drug	Dose (mg kg <sup>-1</sup> )	Administration route	Survival	Date of death
TDMQ20	150	oral	6/6	-
	200	oral	5/5	-
	150	ip	9/11	D3, D15
CQ	150	oral	6/6	-
	200	oral	3/5	D1
	150	ip	4/11	D1

383

### 384 2.4.2. Multiple doses

385 The toxicity of TDMQ20 was then evaluated after on oral administration of 100 mg kg<sup>-1</sup> every  
 386 day to WT C57BL/6J mice. Two mice died at D8 and D9 (survival 8/10), *ie.* after administration  
 387 of 10-11 times the total drug dose used in the AD treatment (80 mg kg<sup>-1</sup> in total). The assay was

388 then discontinued at D9. Mice (n = 9) were then treated with TDMQ20 by oral route at 80 mg kg<sup>-1</sup>  
389 <sup>1</sup>, 3 times a week during 2 weeks, corresponding to a total dose of 480 mg kg<sup>-1</sup>. In these conditions,  
390 with a schedule similar to that used for the evaluation of the pharmacological activity of TDMQ20  
391 (80 mg kg<sup>-1</sup> in total), all mice survived without any detectable sign of toxicity during the treatment,  
392 suggesting a safety index  $\geq 8$ . In addition, the treatment of 5XFAD mice clearly indicated that  
393 this drug-candidate was well tolerated upon long-term oral treatment (45 doses, 450 mg kg<sup>-1</sup> in  
394 total), even in animals weakened by the disease.

395 The aspartate aminotransferase (AST), alanine aminotransferase (ALT), creatinine and urea  
396 were measured in the serum of 5XFAD mice, treated or not by TDMQ20 (45  $\times$  10 mg kg<sup>-1</sup> in 3  
397 months, total dose = 450 mg kg<sup>-1</sup>), at the end of the treatment period and compared to the levels  
398 found in the WT C57BL/6J controls. There was no significant difference between the levels  
399 obtained for the WT controls, the 5XFAD mice and the 5XFAD mice treated by TDMQ20,  
400 indicating the lack of any detectable damage on liver and kidneys upon long-term oral treatment  
401 with TDMQ20 in these conditions (45 doses, 450 mg kg<sup>-1</sup> in total).

402

### 403 **2.4.3. Druggability**

404 *In vitro* preliminary metabolic studies indicate that the TDMQ20 significantly inhibits CYP 2D6,  
405 but not CYP 3A (< 20 %) and 2C9 (< 5 %) (SI). We have to remember that the drug prozac is  
406 also an inhibitor of CYP2D6. The measured pKa values indicate that, at physiological pH,  
407 TDMQ20 should exist as a mixture of species, due to mono- and diprotonation of the side chain,<sup>15</sup>  
408 like many CNS drugs containing protonable nitrogen sites.<sup>38</sup> The calculated log P value for  
409 TDMQ20 is 2.5,<sup>39</sup> and topological polar surface area (tPSA) is 53 Å<sup>2</sup>,<sup>39</sup> in the range consistent for  
410 passive transport across the blood-brain barrier.<sup>38</sup> The membrane crossing capacity has been  
411 confirmed by the Caco-2 data. In standard conditions at 10<sup>-5</sup> M, A-B permeability was 8.4 with  
412 a recovery of 35% and B-A permeability was 10.1 with a recovery of 74%. In addition, TDMQ20  
413 was Ames negative on TA98, TA100, TA1535 and TA1537, even after microsomal activation  
414 (SI), indicating that this ligand was not mutagenic in bacteria.

415

416 In conclusion, TDMQ20 efficiently reversed the cognitive or behavioral impairment using two  
417 non-transgenic mouse models of the early stage of AD and in a transgenic model. With the icv-  
418 CuA $\beta$  and hippo-CuA $\beta$  models, the short-term NOR test is specially robust to evaluate the

419 impairment of the declarative memory in mice, making such models easy to select molecules that  
420 should be active on the early stages of AD.

421 The efficacy of TDMQ20 by oral administration of low doses on three different mouse AD  
422 models is an encouragement for further pharmacological evaluations of this specific copper  
423 chelator.

424

## 425 3. METHODS

426

### 427 3.1. Materials.

428 Human A $\beta$ <sub>1-42</sub> (CF<sub>3</sub>COO<sup>-</sup> as counter-ions) was obtained from Aladdin, China. According to a  
429 protocol adapted from Reference 40, A $\beta$ <sub>1-42</sub> (1 mg) was dissolved in 1,1,1,3,3,3-  
430 hexafluoroisopropanol (HFIP, 1 mL) and sonicated for 15 minutes. The solution was centrifugated  
431 at 12,000 rpm for 15 min. The concentration of the A $\beta$ <sub>1-42</sub> solution was determined using Micro  
432 BCA Protein Assay kit from ThermoFisher Scientific™ (code 23235), working with BSA (bovine  
433 serum albumin) as a calibration protein. HFIP was then removed by lyophilization, and the solid  
434 A $\beta$ <sub>1-42</sub> was then stored at -20 °C until used. The chelators TDMQ20 and TDMQ22 were  
435 synthesized as previously reported.<sup>12,13</sup> Clioquinol (5-chloro-7-iodo-8-hydroxyquinoline, CQ),  
436 CuCl<sub>2</sub>, DMSO and usual chemicals were purchased from Sigma. Phosphate buffered saline 10X  
437 (PBS 10X) was prepared as follows: NaCl 137 mmol, KCl 2.7 mmol, Na<sub>2</sub>HPO<sub>4</sub> 10.0 mmol,  
438 KH<sub>2</sub>PO<sub>4</sub> 1.76 mmol, sterile water qs. 100 mL. PBS 1X was prepared by dilution of PBS 10X in  
439 sterile water. Isoflurane was supplied by Shenzhen RWD life Science Co.

440

### 441 3.2. Animals.

442 Specific pathogen free (SPF) C57 BL/6J mice, weighting at 20–25 g (8 weeks) were purchased  
443 from the Guangdong Medical Experimental Animal Center. 5XFAD mice (strain name: B6.Cg-  
444 Tg(APP<sup>Sw</sup>FILon,PSEN1\*<sup>M146L</sup>\*<sup>L286V</sup>)6799<sup>Vas</sup>/Mmjax), with genetic background C57BL/6  
445 x SJL, were purchased from the Jackson Laboratory (Stock# 34848-JAX|5XFAD, Bar Harbor,  
446 ME, USA) and propagated in the College of Life Sciences and Oceanography in Shenzhen  
447 University. Their offsprings were assessed by PCR detection (Mei5 Biotechnology, China) of the  
448 AD pathogenic genes. Their non-transgenic littermates were screened out as healthy controls.  
449 Animals were separated in groups containing males and females in a 50/50 ratio. They were  
450 housed in standard laboratory conditions: air-conditioned room, temperature 20-25°C, 12 h  
451 light/dark illumination cycle, free access to food and water. Drinking water was distilled water

452 obtained from a Millipore Direct-Q 5 UV water purification system (Millipore SAS, France) and  
453 food was purchased from the Guangdong Medical Experimental Animal Center. Before icv and  
454 intra-hippocampal injections of Cu-A $\beta$ , mice were anesthetized with isoflurane, using a R500  
455 Series Compact Small Animal Anesthesia Machine (Shenzhen RWD Life Science Co.) according  
456 to the supplier instructions. Mice were killed by cervical dislocation after anesthesia with  
457 isoflurane. All animal experiments were conducted in accordance with ethical animal research  
458 standards of the Chinese Council on Animal Care, and approved by the Animal Ethical and  
459 Welfare Committee of Shenzhen University (permit number: AEWC-20140615-002). All efforts  
460 were made to minimize animal suffering.

461

### 462 **3.3. Experimental methods for the icv-CuA $\beta$ and hippo-CuA $\beta$ models.**

#### 463 **3.3.1. Preparation of the Cu-A $\beta_{1-42}$ solution**

464 *Preparation of the A $\beta_{1-42}$  solution.* Human A $\beta_{1-42}$  monomer powder obtained after HFIP treatment  
465 (0.1  $\mu$ mole measured by BCA titration) was dissolved in DMSO (50  $\mu$ L). This mother solution  
466 was then diluted by addition of 200  $\mu$ L of deionized water. The final solution (400  $\mu$ M measured  
467 by BCA assay, H<sub>2</sub>O/DMSO = 80/20, v/v) was stirred using a vortex (1800 rpm, 1 minute) and  
468 sonicated for 1 minute. This limpid solution was aliquoted in seven parts of 30  $\mu$ L each, stored at  
469  $-20$  °C away from light, covered with an aluminum foil (Solution A).

470 *Preparation of the CuCl<sub>2</sub> solution.* A 40 mM stock solution of copper(II) chloride was prepared  
471 by dissolution of CuCl<sub>2</sub> (2.70 mg) in DMSO (500  $\mu$ L). This stock solution was diluted 20 times  
472 in DMSO, to provide a 2 mM solution (Solution B).

473 *Preparation of the Cu-A $\beta_{1-42}$  solution.* The copper-A $\beta_{1-42}$  complex was prepared in a 1/1  
474 metal/peptide ratio, as follows. An aliquot of the human A $\beta_{1-42}$  (above Solution A, 30  $\mu$ L) was  
475 kept at room temperature for 30 min. One mole equivalent of CuCl<sub>2</sub> in DMSO (Solution B, 6  $\mu$ L),  
476 was then added in the flask containing the solution A, the mixture was vortexed for 30 sec, and  
477 then allowed to stand at 37 °C for 15 min. Then, H<sub>2</sub>O (18  $\mu$ L) was added and vortexed, followed  
478 by addition of PBS 10X (6  $\mu$ L), then vortexed for 30 sec. The solution was kept at 37 °C for 15  
479 min. It was again vortexed for 30 sec before each injection in the mouse brains. The absence of  
480 precipitate was carefully checked before each injection. The final ratio H<sub>2</sub>O/DMSO was 80/20,  
481 v/v. This solution (Solution C) was freshly prepared each day, before the intracerebroventricular  
482 (icv-CuA $\beta$  model) or intrahippocampal (hippo-CuA $\beta$  model) injections.

#### 483 **3.3.2. Injection of Cu-A $\beta_{1-42}$ in mouse brain ventricle. (icv-CuA $\beta$ model).**

484 Injections were performed using the protocol adapted from Reference 5. The 35 mice were  
485 randomly assigned to one of the five following groups (7 mice in each group): control mice, mice  
486 which received a single bilateral intracerebroventricular injection of Cu-A $\beta$ <sub>1-42</sub> complex (icv-  
487 CuA $\beta$  group), icv-CuA $\beta$  mice treated with TDMQ20 (TDMQ20 group), icv-CuA $\beta$  mice treated  
488 with TDMQ22 (TDMQ22 group), and icv-CuA $\beta$  mice treated with clioquinol (CQ group). The  
489 intracerebroventricular injections were made at 2 months (mo) of age, with PBS 1X containing  
490 20 vol% of DMSO for the control group, or Cu-A $\beta$ <sub>1-42</sub> Solution C, the four other groups. The  
491 coordinates of the injection sites in each lateral ventricle were: (AP) = - 0.5 mm from bregma;  
492 (L) = +/- 1 mm from bregma; and (D) = - 2.5 mm from skull. The skull was drilled, and an  
493 injector (27 G, 35 mm) was guided successively into the two lateral ventricles, using a mouse  
494 brain localization injector (RWD, Shenzhen, China). Then, 2.5  $\mu$ L of solution C or PBS 1X  
495 containing 20 % DMSO was injected directly into each of the two lateral ventricles (total volume  
496 of injection = 5  $\mu$ L per mouse), using a 5  $\mu$ L syringe mounted on an automated pump. In each  
497 ventricle, the solution was delivered at a rate of 0.5  $\mu$ L/min. After each injection, the injector was  
498 let in place for 5 min to avoid flow back of the solution.

### 499 **3.3.3. Injection of Cu-A $\beta$ <sub>1-42</sub> in mouse hippocampus (hippo-CuA $\beta$ model).**

500 The mice were randomly assigned to one of the four following groups (7 mice in each group):  
501 control mice, mice which received a single bilateral intrahippocampal injection of Cu-A $\beta$ <sub>1-42</sub>  
502 complex (hippo-CuA $\beta$ ), hippo-CuA $\beta$  mice treated with TDMQ20, hippo-CuA $\beta$  mice treated with  
503 clioquinol (CQ group). The injections in the two CA3 hippocampus regions were made at 2  
504 months of age, with PBS 1X containing 20 vol% of DMSO for the control group, or Cu-A $\beta$ <sub>1-42</sub>  
505 Solution C, for the three other groups. The coordinates of the injection sites were: (AP) = -2.18  
506 mm from bregma; (L) = +/- 2.3 mm from bregma; and (D) = - 2.15 mm from skull. The skull  
507 was drilled, and an injector (27 G, 35 mm) was guided successively into the bilateral CA3  
508 hippocampal regions. The delivery of the Cu-A $\beta$ <sub>1-42</sub> (solution C, 2 x 2.5  $\mu$ L of the Cu-A $\beta$ <sub>1-42</sub>  
509 solution C, or the PBS 1X/DMSO, 80/20, v/v into the bilateral hippocampal CA3 region was  
510 carried out in the same way than icv injections, except that the flow rate was 0.25  $\mu$ L/min  
511 (compared to 0.5  $\mu$ L/min for cerebroventricular space, in order to avoid damage to the smaller  
512 hippocampus).

### 513 **3.3.4. Preparation of drug solutions, drug dose, and treatment.**

514 Mother solutions of TDMQ20, TDMQ22 were prepared by dissolving 25 mg of each drug in 10  
515 mL of NaCl 0.9 % (w/v) solution. Clioquinol (25 mg) was dissolved in 10 mL of DMSO. 100  $\mu$ L



516 of such drug solutions contained 0.25 mg of drug. While the injections of Cu-A $\beta$ <sub>1-42</sub> into ventricles  
517 or hippocampus were carried out on D0, the mice were treated intragastrically 8 times (at D4, D6,  
518 D9, D11, D13, D16, D18, and D20) as follows: NaCl 0.9% (w/v) in distilled water (100  $\mu$ L) for  
519 the control groups, the icv-CuA $\beta$  group, and the hippo-CuA $\beta$  group, TDMQ20 in NaCl 0.9 %  
520 (100  $\mu$ L) for the TDMQ20 groups, TDMQ22 in NaCl 0.9% (100  $\mu$ L) for the TDMQ22 groups,  
521 and CQ in DMSO (100  $\mu$ L) for the CQ group. Each drug dose was therefore 10 mg kg<sup>-1</sup> for  
522 TDMQ20, TDMQ22, and CQ. Mice were individually weighted on the day of the intracerebral  
523 injection of Cu-A $\beta$  (2 months of age) for the icv-CuA $\beta$ - and hippo-CuA $\beta$  models, and the exact  
524 volume of drug solution for each mouse was calculated accordingly. For 5XFAD mice, animals  
525 were weighted at the age of two months (beginning of treatment) and the volumes of drug  
526 solutions were calculated accordingly.

527

### 528 **3.4. Experimental methods for the 5XFAD transgenic model.**

529 At the age of 2 months, mice were weighted and randomly assigned to one of the following  
530 groups: untreated 5XFAD mice, 5XFAD mice treated with TDMQ20, 5XFAD mice treated with  
531 CQ, compared to wild type C57BL/6 x SJL mice. The drugs were dissolved in 0.9% NaCl  
532 (TDMQ20) or DMSO (CQ), and were delivered to the stomach of mice once every two days  
533 during the three following months (45 treatments, total drug dose: 450 mg kg<sup>-1</sup>). Each drug dose  
534 consisted of 10 mg kg<sup>-1</sup> of mouse weight contained in 100  $\mu$ L of solvent. All control and untreated  
535 mice received oral gavage with aqueous NaCl 0.9% instead of drug. The behavioral tests were  
536 performed at the end of the treatment, between 5.0 and 5.5 months of age.

537

### 538 **3.5. Behavioral tests.**

#### 539 **3.5.1. Novel object recognition test (NOR).**

540 The test was carried out as previously reported.<sup>28</sup> Mice were tested in an uncovered square box  
541 (40 cm  $\times$  40 cm  $\times$  40 cm). This open arena is divided into 25 equal squares. At D22 after the  
542 injection of Cu-A $\beta$  in the ventricles or hippocampus (two days after the last administration of  
543 drug), each mouse was placed for 5 min in the empty arena of the box placed in the test room  
544 equipped with daylight lamp, in order to habituate it to the environment and to the apparatus  
545 (habituation phase). At D23, the home cages were left for acclimation in the test room for one  
546 hour prior to the beginning of the test session (acclimation phase). Each mouse was then placed  
547 for 5 min in the arena containing two identical objects (X and X') (acquisition phase). After a 90

548 min retention interval in its home cage, the mouse was placed back into the arena and exposed to  
549 one of the familiar objects (X) and to a novel object (Y), for a short-term (90 min) recognition  
550 memory test. The mouse was initially placed in the apparatus facing the wall and allowed to  
551 explore the objects for 5 min. When the mouse's nose pointed or touched an object within 1 cm,  
552 it was recorded as an exploration behavior. The number of times the mouse explored one of the  
553 two objects was recorded. At D24, each mouse was similarly placed into the arena for 5 min, in  
554 the presence of a different pair of dissimilar objects (a familiar and a novel one; X and Z,  
555 respectively), for a long-term (1 day) recognition memory test. The recognition index, defined as  
556 the ratio of the number of times the novel object was explored to the number of times both objects  
557 were explored, was used to measure the memory function. So, the recognition indexes were  
558 calculated as  $n_Y/n_{(X+Y)}$  and  $n_Z/n_{(X+Z)}$  for the short-term memory and long-term memory,  
559 respectively, where  $n_X$ ,  $n_Y$ ,  $n_Z$  stand for the number of explorations of objects X, Y or Z,  
560 respectively. Between trials, the arena was cleaned with 75% ethanol to eliminate animal clues,  
561 and then with water. For the 5XFAD mice, the schedule of the test was the same as described  
562 above, and the test begun at  $5.3 \pm 0.1$  months of age.

### 563 **3.5.2. Elevated plus maze test (EPM).**

564 The elevated plus maze test was carried out using the protocol adapted from References 41 and  
565 42. The experiment was started at D26 from intracerebral injection. The home cages were left for  
566 acclimation in the test room equipped with daylight lamp, for one hour prior to the beginning of  
567 the test session. The elevated plus maze apparatus consisted of four arms of 30 cm length  $\times$  5 cm  
568 width, two of them with 30 cm high walls, elevated at 60 cm above the floor. The mouse was  
569 initially placed in the center of the maze, facing an open arm and allowed to explore the maze for  
570 5 min. The number of times the mouse entered the open and closed arms was recorded, as well as  
571 the time spent in the open and closed arms. If the mouse fell off an open arm, the trial was stopped  
572 and excluded from the analysis. For 5XFAD mice, the test was carried out at  $5.4 \pm 0.1$  mo. of age.  
573 Between trials, the arena was cleaned with 75% ethanol to eliminate animal clues, and then with  
574 water.

### 575 **3.5.3. Open field test (OFT).**

576 The test was carried out at D26 after intracerebral injection, using the protocol adapted from  
577 References 43 and 44. The home cages were left for acclimation in the test room equipped with  
578 daylight lamp, for one hour prior to the beginning of the test session. The test field consisted of  
579 an empty square box of  $100 \times 100 \times 30$  cm, with 25 square grids on the floor. Each mouse was

580 initially put at the center of the field, and allowed to explore it for 5 min. A digital camera was  
581 placed 2 m above and its field of view covered the entire experimental field. The number of  
582 rearings, crossings of the floor grid, and walking distances of mice were recorded. For 5XFAD  
583 mice, the test was carried out at  $5.4 \pm 0.1$  months of age.

#### 584 **3.5.4. Y-maze test (YMT).**

585 The Y-maze test was carried out using the protocol adapted from Reference 45. The home cages  
586 were left for acclimation in the test room equipped with daylight lamp, for one hour prior to the  
587 beginning of the test session. Spontaneous alternation behavior test has been performed in a  
588 symmetrical black plexiglas Y-maze with three arms (30 cm long  $\times$  10 cm wide  $\times$  30 cm high) at  
589  $120^\circ$  angles. For 5XFAD mice, the test was carried out at  $5.5 \pm 0.1$  months of age. The mice were  
590 initially placed in the center of the maze and allowed to explore the maze for 5 min. A successful  
591 alternation was defined as any three consecutive choices of three different arms without re-  
592 exploration of a previously visited arm. Alternation rate (%) was calculated as follows: number  
593 of triads containing entries into all three arms/maximum possible alternations (the total number  
594 of arms entered  $- 2$ ) $\times 100$ .

595

### 596 **3.6. Biochemical analyses.**

#### 597 **3.6.1. Titration of malondialdehyde (MDA).**

598 After all behavioral experiments have been performed, all the mice had a rest for one day and then  
599 were sacrificed. The concentration of malondialdehyde (MDA) was determined in cortex of C57  
600 BL/6J control mice, and icv-CuA $\beta$  mice  $\pm$  TDMQ20 or CQ, using the thiobarbituric assay  
601 according to the manufacturer's instructions (Nanjing Jiancheng Bioengineering Institute, China).  
602 The cortex (*ca.* 100 mg was homogenized in 1 mL of phosphate buffer (pH 7.4, 10 mM). After  
603 centrifugation for 10 min (3,000 g), the MDA content in the supernatant was measured by UV-  
604 visible spectrometry at 532 nm. The levels of MDA are indicated as nmol/mg protein.

#### 605 **3.6.2. Titration of AST, ALT, creatinine and urea.**

606 After all behavioral experiments have been performed, all 5XFAD mice had a rest for one day  
607 and then were sacrificed (5.6 months of age). The concentration of AST, ALT, creatinine and urea  
608 in the serum were measured using the automatic biochemical analyzer iMagic-M7, the assay kits  
609 and the software of the iCubio company (Shenzhen, China).

610

### 611 **3.7. Preliminary toxicologic experiments**

612 **3.7.1. Single dose (acute toxicity).**

613 TDMQ20 and CQ were administered by gavage or by intraperitoneal injection, at 150 or 200 mg  
614 kg<sup>-1</sup>, to C57 BL/6J mice (groups of 5-11 mice each), using 25 mg mL<sup>-1</sup> solutions in 0.9% NaCl  
615 (for TDMQ20) or in DMSO (for CQ). Mice were observed for 16 days after the administration.

616 **3.7.2. Multiple doses.**

617 C57 BL/6J mice received TDMQ20 (25 mg mL<sup>-1</sup> solution in 0.9% NaCl) by intragastric  
618 administration at 100 mg kg<sup>-1</sup> per day during 9 days (10 mice), or at 60 mg kg<sup>-1</sup> per day, three  
619 times per week during two weeks (12 mice). Mice were weighted each day.

620

621 **3.8. Statistical analysis.**

622 Figures 2-6 and Figure S1 are presented as univariate scatterplots of all the individual data points  
623 obtained, with mean and SEM superimposed. Data with multiple independent experiments were  
624 analyzed by one-way ANOVA, followed by multiple comparisons LSD test when the ANOVA  
625 was significant ( $p < 0.05$ ).  $p$ -levels  $< 0.05$ ,  $0.01$  and  $< 0.001$  were noted \*, \*\* and \*\*\*,  
626 respectively. For each test, each mice was evaluated only once (no repeated measures). The factor  
627 of the treatment was entered as a within-subjects (independent) factor. The F-statistic, degrees of  
628 freedom,  $p$ -value and the magnitude of the difference were calculated. All statistical calculations  
629 are provided as Supporting Information (SI).

630

631 ASSOCIATED CONTENT

632 The Supporting Information is available free of charge at <https://pubs.acs.org/doi/...>

633 The Supporting Information contain:

- 634 - Figure S1 (duplicate of Figure 2),  
635 - Raw data and statistical analysis of results reported in Figures 2-6,  
636 - ADME-toxicological data of TDMQ20.

637

638 AUTHOR INFORMATION

639 **Corresponding Authors**

640 Anne Robert – Laboratoire de Chimie de Coordination du CNRS (LCC-CNRS), 205 route de  
641 Narbonne, 31077 Toulouse, cedex 4, France; [orcid.org/0000-0002-9092-6776](https://orcid.org/0000-0002-9092-6776); [anne.robert@lcc-](mailto:anne.robert@lcc-toulouse.fr)  
642 [toulouse.fr](mailto:anne.robert@lcc-toulouse.fr)

643 Qiong Liu – College of Life Sciences & Oceanography, Shenzhen University, 1066 Xueyuan  
644 boulevard, Nanshan District, Shenzhen 518055, P. R. China; orcid.org/0000-0002-6431-3650;  
645 liuqiong@szu.edu.cn

646 Bernard Meunier – Laboratoire de Chimie de Coordination du CNRS (LCC-CNRS), 205 route de  
647 Narbonne, 31077 Toulouse, cedex 4, France, and School of Chemical Engineering and Light  
648 Industry, Guangdong University of Technology (GDUT), Higher Education Mega Center, 100  
649 Waihuan Xi road, Panyu District, Guangzhou 510006, P. R. China; orcid.org/0000-0003-2200-  
650 7142; bmeunier@lcc-toulouse.fr

651

### 652 **Other Authors**

653 Jie Zhao – College of Life Sciences & Oceanography, Shenzhen University, 1066 Xueyuan  
654 boulevard, Nanshan District, Shenzhen 518055, P. R. China, and College of Optoelectronic  
655 Engineering, Shenzhen University, Shenzhen 518060, China; orcid.org/0000-0002-7878-9801.

656 Qihui Shi – College of Life Sciences & Oceanography, Shenzhen University, 1066 Xueyuan  
657 boulevard, Nanshan District, Shenzhen 518055, P. R. China; orcid.org/0000-0002-7172-7368.

658 Hongda Tian – School of Chemical Engineering and Light Industry, Guangdong University of  
659 Technology (GDUT), Higher Education Mega Center, 100 Waihuan Xi road, Panyu District,  
660 Guangzhou 510006, P. R. China.

661 Youzhi Li – School of Chemical Engineering and Light Industry, Guangdong University of  
662 Technology (GDUT), Higher Education Mega Center, 100 Waihuan Xi road, Panyu District,  
663 Guangzhou 510006, P. R. China.

664 Yan Liu – School of Chemical Engineering and Light Industry, Guangdong University of  
665 Technology (GDUT), Higher Education Mega Center, 100 Waihuan Xi road, Panyu District,  
666 Guangzhou 510006, P. R. China; orcid.org/0000-0002-3864-1992.

667 Zhen Xu – Shenzhen Institutes of Advanced Technology, Chinese Academy of Sciences,  
668 Shenzhen 518055, China.

669

### 670 **Author Contributions**

671 B. M., Q. L. and A. R. designed research; H. T., Y. Li and Y. Liu performed chelator synthesis;  
672 J. Z. and Q. S. performed biological assays and animal experiments; B. M., Q. L., J. Z. and A. R.  
673 analyzed the data; B. M., A. R. and Q. L. wrote the manuscript.

674

675 **Funding Sources**

676 This work was financially supported by the Guangdong Provincial Key S&T Program  
677 (2018B030336001), NSFC (grants 21977019 and 21877081), the Guangdong Province (Program  
678 for Innovative Research Teams and Leading Talents Introduction, grant 2050205), the Open  
679 Project of Guangdong Provincial Key Laboratory of New Drug Screening (No.GDKLNDS-  
680 2018OF004), and the University of Technology of the Guangdong (GDUT) (grant 220418037) of  
681 the P. R. China, and by the CNRS, France.

682

683 **Conflict of Interest**

684 Y. L., A. R. and B. M. are co-authors of a pending patent on use of TDMQ chelators as a  
685 therapeutic for Alzheimer's disease (WO 2017/202360 A1). None of the authors have a financial  
686 interest in pharmaceutical companies.

687

688 **REFERENCES**

689

- 690 1. WHO. Data on AD. (2019). Retrieved from [https://www.who.int/news-room/fact-](https://www.who.int/news-room/fact-sheets/detail/dementia)  
691 [sheets/detail/dementia](https://www.who.int/news-room/fact-sheets/detail/dementia). Accessed September 8, 2020.
- 692 2. Meunier, B. (2016). Age and Alzheimer's disease. *Nutrients*, 8, 372.
- 693 3. Wang, X., Sun, G., Feng, T., Zhang, J., Huang, X., Wang, T., Xie, Z., Chu, X., Yang, J.,  
694 Wang, H., Chang, S., Gong, Y., Ruan, L., Zhang, G., Yan, S., Lian, W., Du, C., Yang, D.,  
695 Zhang, Q., Lin, F., Liu, J., Zhang, H., Ge, C., Xiao, S., Ding, J., Geng, M. (2019). Sodium  
696 oligomannate therapeutically remodels gut microbiota and suppress gut bacterial amino  
697 acids-shaped neuroinflammation to inhibit Alzheimer's disease progression. *Cell Res.*, 29,  
698 787-803.
- 699 4. Cummings, J. L., Morstorf, T., Zhong, K. (2014). Alzheimer's disease drug-development  
700 pipeline: few candidates, frequent failures. *Alzheimer's Res. Ther.*, 6, 37-43.
- 701 5. Ceccom, J., Coslédan, F., Halley, H., Francès, B., Lassalle, J.-M., Meunier, B. (2012). Copper  
702 chelator induced efficient episodic memory recovery in a non-transgenic mouse model. *Plos*  
703 *One*, 7, e43105.
- 704 6. Selkoe, D. J., Hardy, J. (2016). The amyloid hypothesis of Alzheimer's disease at 25 years.  
705 *EMBO Mol. Med.*, 8, 595-608.

- 706 7. Tomiyama, T., Matsuyama, S., Iso, H., Umeda, T., Takuma, H., Ohnishi, K., Ishibashi, K.,  
707 Teraoka, R., Sakama, N., Yamashita, T., Nishitsuji, K., Ito, K., Shimada, H., Lambert, M. P.,  
708 Klein, W. L., Mori, H. (2010). A mouse model of amyloid  $\beta$  oligomers: Their contribution to  
709 synaptic alteration, abnormal tau phosphorylation, glial activation and neuronal loss *in vivo*. *J.*  
710 *Neurosci*, *30*, 4845-4856.
- 711 8. Zhang, F., Gannon, M., Chen, Y., Yan, S., Zhang, S., Feng, W., Tao, J., Sha, B., Liu, Z.,  
712 Saito, T., Saido, T., Keene, C. D., Jiao, K., Roberson, E. D., Xu, H., Wang, Q. (2020).  $\beta$ -  
713 amyloid redirects norepinephrine signaling to activate the pathogenic GSK3 $\beta$ /tau cascade.  
714 *Sci. Transl. Med.*, *12*, eaay6931.
- 715 9. Nguyen, M., Robert, A., Sournia-Saquet, A., Vendier, L., Meunier, B. (2014).  
716 Characterization of new specific copper chelators as potential drugs for the treatment of  
717 Alzheimer's disease. *Chem. Eur. J.*, *20*, 6771-6785.
- 718 10. Nguyen, M., Bijani, C., Martins, N., Meunier, B., Robert, A. (2015). Transfer of copper from  
719 an amyloid to a natural copper-carrier peptide with a specific mediating ligand. *Chem. Eur.*  
720 *J.*, *21*, 17085-17090.
- 721 11. Liu, Y., Nguyen, M., Robert, A., Meunier, B. (2019). Metals ions in Alzheimer's disease: a  
722 key role or not? *Acc. Chem. Res.*, *52*, 2026-2035, and references therein.
- 723 12. Zhang, W., Huang, M., Bijani, C., Liu, Y., Robert, A., Meunier, B. (2018). Synthesis and  
724 characterization of copper specific tetradentate ligands as potential treatment for Alzheimer's  
725 disease. *C. R. Chimie*, *21*, 475-483.
- 726 13. Zhang, W., Huang, D., Huang, M., Huang, J., Wang, D., Liu, X., Nguyen, M., Vendier, L.,  
727 Mazères, S., Robert, A., Liu, Y., Meunier, B. (2018). Preparation of new tetradentate copper  
728 chelators as potential anti-Alzheimer agents. *ChemMedChem*, *13*, 684-704.
- 729 14. Huang, J., Nguyen, M., Liu, Y., Robert, A., Meunier, B. (2019). The TDMQ regulators of  
730 copper homeostasis do not disturb Cu,Zn-SOD and tyrosinase activity, nor the Co(III)  
731 cofactor vitamin B12. *Eur. J. Inorg. Chem.*, 1384-1388.
- 732 15. Li, Y., Nguyen, M., Baudoin, M., Vendier, L., Liu, Y., Robert, A., Meunier, B. (2019). Why  
733 is tetradentate coordination essential for potential copper homeostasis regulators in  
734 Alzheimer's disease? *Eur. J. Inorg. Chem.*, 4712-4718.
- 735 16. Adlard, P. A., Bush, A. I. (2018). Metal and Alzheimer's disease: How far have we come in  
736 the clinic? *J. Alz. Dis.*, *62*, 1369-1379.

- 737 17. Prana Biotechnology announces preliminary results of Phase 2 IMAGINE trial of PBT2 in  
738 Alzheimer's disease. (2014). Retrieved from [https://www.prnewswire.com/news-](https://www.prnewswire.com/news-releases/prana-biotechnology-announces-preliminary-results-of-phase-2-imagine-trial-of-pbt2-in-alzheimers-disease-253173581.html)  
739 [releases/prana-biotechnology-announces-preliminary-results-of-phase-2-imagine-trial-of-](https://www.prnewswire.com/news-releases/prana-biotechnology-announces-preliminary-results-of-phase-2-imagine-trial-of-pbt2-in-alzheimers-disease-253173581.html)  
740 [pbt2-in-alzheimers-disease-253173581.html](https://www.prnewswire.com/news-releases/prana-biotechnology-announces-preliminary-results-of-phase-2-imagine-trial-of-pbt2-in-alzheimers-disease-253173581.html). Accessed September 8, 2020.
- 741 18. Nguyen, M., Rechinat, L., Robert, A., Meunier, B. (2015). The necessity of having a  
742 tetradentate ligand to extract copper(II) ions from amyloids. *ChemistryOpen*, 4, 27-31.
- 743 19. Nguyen, M., Vendier, L., Stigliani, J. -L., Meunier, B., Robert, A. (2017). Structures of  
744 copper and zinc complexes of PBT2, a chelating agent evaluated as potential drug for  
745 neurodegenerative diseases. *Eur. J. Inorg. Chem.*, 600-608.
- 746 20. Zhang, W., Liu, Y., Hureau, C., Robert, A., Meunier, B. (2018). N4-Tetradentate chelators  
747 efficiently regulate copper homeostasis and prevent ROS production induced by copper-  
748 amyloid, even in the presence of an excess of zinc. *Chem. Eur. J.*, 24, 7825-7829.
- 749 21. West, M. J. (1993). Regionally specific loss of neurons in aging human hippocampus.  
750 *Neurobiol. Aging*, 14, 287-293.
- 751 22. Mu, Y., Gage, F. H. (2011). Adult hippocampal neurogenesis and its role in Alzheimer's  
752 disease. *Molec. Neurodegener.*, 6, 85.
- 753 23. Halliday, G. (2017). Pathology and hippocampal atrophy in Alzheimer's disease. *Lancet*  
754 *Neurol.*, 16, 862-864.
- 755 24. Oakley, H., Cole, S. L., Logan, S., Maus, E., Shao, P., Craft, J., Guillozet-Bongaarts, A.,  
756 Ohno, M., Disterhoft, J., Van Eldik, L., Berry R., Vassar, R. (2006). Intraneuronal  $\beta$ -amyloid  
757 aggregates, neurodegeneration, and neuron loss in transgenic mice with five familial  
758 Alzheimer's disease mutations: Potential factors in amyloid plaque formation, *J. Neurosci.*,  
759 26, 10129-10140.
- 760 25. Jawhar, S., Trawicka, A., Jenneckens, C., Bayer, T. A., Wirths, O. (2012). Motor deficits,  
761 neuron loss, and reduced anxiety coinciding with axonal degeneration and intraneuronal A $\beta$   
762 aggregation in the 5XFAD mouse model of Alzheimer's disease. *Neurobiol. Aging*, 33,  
763 196.e29-196.e40.
- 764 26. Schneider, F., Baldauf, K., Wetzel, W., Reymann, K. G. (2014). Behavioral and EEC changes  
765 in male 5xFAD mice. *Physiol. Behav.*, 135, 25-33.
- 766 27. Urano, T., Tohda, C. (2010). Icarin improves memory impairment in Alzheimer's disease  
767 model mice (5xFAD) and attenuates amyloid  $\beta$ -induced neurite atrophy. *Phytother. Res.*, 24,  
768 1658-1663.



- 769 28. Morroni, F., Sita, G., Tarozzi, A., Rimondini, R., Hrelia, P. (2016). Early effects of A $\beta$ <sub>1-42</sub>  
770 oligomers injection in mice: involvement of PI3K/Akt/GSK3 and MAPK/ERK1/2 pathways.  
771 *Behav. Brain Res.*, 314, 106-115.
- 772 29. Grayson, B., Leger, M., Piercy, C., Adamson, L., Harte, M., Neill, J. C. (2015). Assessment  
773 of disease-related cognitive impairments using the novel object recognition (NOR) task in  
774 rodents. *Behav. Brain Res.*, 285, 176-193.
- 775 30. Ardestani, P. M., Evans, A. K., Yi, B., Nguyen, T., Coutellier, L., Shamloo, M. (2017).  
776 Modulation of neuroinflammation and pathology in the 5XFAD mouse model of Alzheimer's  
777 disease using a biased and selective beta-1 adrenergic receptor partial agonist.  
778 *Neuropharmacol.*, 116, 371-386.
- 779 31. Kraeuter, A. K., Guest, P. C., Sarnyai, Z. (2019). The Y-maze for assessment of spatial  
780 working and reference memory in mice. *Methods Mol. Biol.*, 1916, 105-111.
- 781 32. Conrad, C. D., Galea, L. A. M., Kuroda, Y., McEwen, B. S. (1996). Chronic stress impairs  
782 rat spatial memory on the Y maze, and this effect is blocked by tianeptine pretreatment.  
783 *Behav. Neurosci.*, 110, 1321-1334.
- 784 33. Ohno, M., Sametsky, E. A., Younkin, L. A., Oakley, H., Younkin, S. G., Citron, M., Vassar,  
785 R., Disterhoft, J. F. (2004). BACE1 deficiency rescues memory deficits and cholinergic  
786 dysfunction in a mouse model of Alzheimer's disease. *Neuron*, 41, 27-33.
- 787 34. File, S. E. (2001). Factors controlling measures of anxiety and responses to novelty in the  
788 mouse. *Behav. Brain Res.*, 125, 151-157.
- 789 35. Walf, A. A., Frye, C. A. (2007). The use of the elevated plus maze as an assay of anxiety-  
790 related behavior in rodents. *Nat. Protoc.*, 2, 322-328.
- 791 36. Webster, S. J., Bachstetter, A. D., Van Eldik, L. J. (2013). Comprehensive behavioral  
792 characterization of an APP/PS-1 double knock-in mouse model of Alzheimer's disease.  
793 *Alzheimer Res. Ther.*, 5, 28.
- 794 37. Tsikas, D. (2017). Assessment of lipid peroxidation by measuring malondialdehyde (MDA)  
795 and relatives in biological samples: analytical and biological challenges. *Anal. Biochem.*, 524,  
796 13-30.
- 797 38. Pajouhesh, H., Lenz, G. R. (2005). Medicinal chemical properties of successful central  
798 nervous system drugs. *NeuroRx*, 2, 541-553.
- 799 39. ChemDraw Prime software, version 19.0.0.26.

- 800 40. Zhang, C., Wan, X., Zheng, X., Shao, X., Liu, Q., Zhang, Q., Qian, Y. (2014). Dual-functional  
801 nanoparticulates targeting amyloid plaques in the brains of Alzheimer's disease mice.  
802 *Biomaterials*, *35*, 456-464.
- 803 41. Lister, R. G. (1987). The use of a plus-maze to measure anxiety in the mouse.  
804 *Psychopharmacology*, *92*, 180-185.
- 805 42. JiaWen, W., Hong, S., ShengXiang, X., Jing, L. (2018). Depression- and anxiety-like  
806 behaviour is related to BDNF/TrkB signalling in a mouse model of psoriasis. *Clin. Exp.*  
807 *Dermatol.*, *43*, 254-261.
- 808 43. Garcez, M. L., Mina, F., Bellettini-Santos, T., da Luz, A. P., Schiavo, G. L., Carollo Macieski,  
809 J. M., Behenck Medeiros, E., Oliveira Marques, A., Quadros Magnus, N., Budni, J. (2018).  
810 The involvement of nlrp3 on the effects of minocycline in an ad-like pathology induced by  
811  $\beta$ -amyloid oligomers administered to mice. *Mol. Neurobiol.*, *56*, 2606-2617.
- 812 44. Xie, Y., Liu, Q., Zheng, L., Wang, B., Qu, X., Ni, J., Zhang, Y., Du, X. (2018). Se-  
813 Methylselenocysteine ameliorates neuropathology and cognitive deficits by attenuating  
814 oxidative stress and metal dyshomeostasis in Alzheimer model mice. *Mol. Nutr. Food Res.*,  
815 *62*, e1800107.
- 816 45. Takagane, K., Nojima, J., Mitsunashi, H., Suo, S., Yanagihara, D., Takaiwa, F., Urano, Y.,  
817 Noguchi, N., Ishiura, S. (2015). A $\beta$  induces oxidative stress in senescence-accelerated  
818 (SAMP8) mice. *Biosc. Biotech. Biochem.*, *79*, 912-918.
- 819  
820

821 **Scheme for Table of Contents only**

822

823

